





## Article

# The Potential of GRASP/GARRLiC Retrievals for Dust Aerosol Model Evaluation: Case Study during the PreTECT Campaign

Dimitra Konsta <sup>1,\*</sup>, Alexandra Tsekeri <sup>2</sup>, Stavros Solomos <sup>2,3</sup>, Nikolaos Siomos <sup>2,4</sup>, Anna Gialitaki <sup>2,4</sup> , Eleni Tetoni <sup>2,5</sup> , Anton Lopatin <sup>6</sup>, Philippe Goloub <sup>7</sup>, Oleg Dubovik <sup>7</sup> , Vassilis Amiridis <sup>2</sup> and Panagiotis Nastos <sup>1</sup> 

- <sup>1</sup> Laboratory of Climatology & Atmospheric Environment, Faculty of Geology and Geoenvironment, National and Kapodistrian University of Athens, University Campus, GR-15784 Athens, Greece; nastos@geol.uoa.gr
- <sup>2</sup> Institute for Astronomy, Astrophysics, Space Applications and Remote Sensing, National Observatory of Athens, I. Metaxa & Vas. Pavlou Penteli, GR-15236 Nea Penteli Attica, Greece; atsekeri@noa.gr (A.T.); stavros@noa.gr (S.S.); nsiomos@noa.gr (N.S.); togialitaki@noa.gr (A.G.); eleni.tetoni@dlr.de (E.T.); vamoir@noa.gr (V.A.)
- <sup>3</sup> Research Centre for Atmospheric Physics and Climatology, Academy of Athens, 84 Solonos St., GR-10680 Athens, Greece
- <sup>4</sup> Laboratory of Atmospheric Physics, Physics Department, Aristotle University of Thessaloniki, GR-54124 Thessaloniki, Greece
- <sup>5</sup> Institute of Atmospheric Physics, German Aerospace Center (DLR), Münchner Str. 20, 82234 Oberpfaffenhofen, Germany
- <sup>6</sup> GRASP SAS, 59650 Villeneuve d'Ascq, France; anton.lopatin@grasp-sas.com
- <sup>7</sup> UMR 8518-LOA-Laboratoire d'Optique Atmosphérique, CNRS, University Lille, 59000 Lille, France; philippe.goloub@univ-lille.fr (P.G.); oleg.dubovik@univ-lille.fr (O.D.)
- \* Correspondence: dkonsta@noa.gr



**Citation:** Konsta, D.; Tsekeri, A.; Solomos, S.; Siomos, N.; Gialitaki, A.; Tetoni, E.; Lopatin, A.; Goloub, P.; Dubovik, O.; Amiridis, V.; et al. The Potential of GRASP/GARRLiC Retrievals for Dust Aerosol Model Evaluation: Case Study during the PreTECT Campaign. *Remote Sens.* **2021**, *13*, 873. <https://doi.org/10.3390/rs13050873>

Academic Editors:  
Alexander Kokhanovsky and  
Gerrit de Leeuw

Received: 29 December 2020  
Accepted: 23 February 2021  
Published: 26 February 2021

**Publisher's Note:** MDPI stays neutral with regard to jurisdictional claims in published maps and institutional affiliations.



**Copyright:** © 2021 by the authors. Licensee MDPI, Basel, Switzerland. This article is an open access article distributed under the terms and conditions of the Creative Commons Attribution (CC BY) license (<https://creativecommons.org/licenses/by/4.0/>).

**Abstract:** We use the Generalized Retrieval of Aerosol Surface Properties algorithm (GRASP) to compare with dust concentration profiles derived from the NMME-DREAM model for a specific dust episode. The GRASP algorithm provides the possibility of deriving columnar and vertically-resolved aerosol properties from a combination of lidar and sun-photometer observations. Herein, we apply GRASP for analysis of a Saharan dust outburst observed during the “PREparatory: does dust TriboElectrification affect our ClimaTe” campaign (PreTECT) that took place at the North coast of Crete, at the Finokalia ACTRIS station. GRASP provides column-averaged and vertically resolved microphysical and optical properties of the particles. The retrieved dust concentration profiles are compared with modeled concentration profiles derived from the NMME-DREAM dust model. To strengthen the results, we use dust concentration profiles from the Polarization-Lidar PHOTometer Networking method (POLIPHON). A strong underestimation of the maximum dust concentration is observed from the NMME-DREAM model. The reported differences between the retrievals and the model indicate a high potential of the GRASP algorithm for future studies of dust model evaluation.

**Keywords:** GRASP/GARRLiC retrieval algorithm; aerosol properties; dust model evaluation

## 1. Introduction

Desert dust is one of the most dominant aerosol types on Earth, produced in arid regions. Windblown dust particles can have a significant climate impact since they can cover great distances from their sources, directly affecting the planetary radiative balance through their interaction with solar and terrestrial radiation [1] and indirectly influencing cloud formation and cloud optical properties [2]. Dust also affects the prevailing atmospheric conditions and air quality in the transported areas (i.e., the Mediterranean Sea and Europe), thus affecting the health of large populations, especially when synoptic conditions favor its advection within the boundary layer [3–6].

One of the largest sources of dust particles is the Sahara region, which transports dust throughout the year towards the Mediterranean Sea. The dust aerosols strongly

affect the Mediterranean Sea and South Europe, since they can travel over long distances with varying residence times depending on the meteorological conditions [7–9]. In spring, Saharan dust transported from the north African coast towards the Mediterranean is very often driven by the south “Khamsin” winds [10].

Airborne dust particles, as well as other aerosol types, can be identified and characterized by ground-based passive and active remote sensing sensors. For example, passive remote sensing measurements are performed with multi-wavelength sun-photometers and are used to provide the column-integrated properties of aerosol particles [11,12]. Active remote sensing measurements with multi-wavelength lidar systems provide high-resolution profiles of aerosol properties (i.e., aerosol backscatter and extinction coefficient profiles) [13–15]. The combination of the sun-photometers with lidar measurements enhances the observational information content towards aerosol characterization [16–18]. To this end, retrieval algorithms that benefit from collocated active and passive remote sensing measurements have been developed.

One of examples of such an approach is the Generalized Aerosol Retrieval from Radiometric and Lidar Combination (GARRLiC) retrieval [18] developed as a part of the rather extensive Generalized Retrieval of Atmosphere and Surface Properties (GRASP) algorithm [12,19]: Building on the heritage of the AERONET retrieval, GRASP/GARRLiC can process only passive radiometric and also active lidar observations. Specifically, it can be applied to a combined lidar and sun-photometer measurements and derive both vertically resolved and columnar information about aerosol particles [18]. The detailed capabilities and evolution of GRASP/GARRLiC algorithm is discussed in [20].

GRASP/GARRLiC has been successfully applied in the past for the characterization of Sahara dust particles [21] and their diurnal cycles [20,22] as well as aerosol mixtures, e.g., for dust and smoke [18] and for dust and marine particles [23]. For example, comparison of the GRASP/GARRLiC results with modelled dust concentration profiles revealed a strong underestimation by the model but a good agreement in terms of the profile structure [23]. Good agreement was also found from a comparison with air-borne in-situ measurements of dust concentrations [24–26]. For ground-based in-situ measurements the comparison was more challenging due to limited information provided by lidar systems in the lowermost part of the atmosphere (the lidar incomplete overlap region) [23], while in [24] the differences in the extinction coefficient vertical profiles retrieved by GRASP/GARRLiC and calculated with the Raman technique are below 30%. The latest version of the GRASP source code is available for download at <https://www.grasp-open.com/products/> (accessed on 29 December 2020).

Dust models are an important tool to refine our knowledge on the dust cycle: the amount of dust emitted from the sources, transported, and deposited. Several studies have evaluated dust models and found a large diversity in the burdens of the simulated dust [23,27–31], revealing large uncertainties in simulated dust processes (e.g., transport). It is thus imperative that models are regularly tested against observations to evaluate their ability to accurately represent dust cycles in the atmosphere.

Thus, the objective of the present study is twofold. First, using the lidar/sun-photometer measurements to apply the GRASP/GARRLiC inversion algorithm for the characterization of a Saharan dust outbreak observed in the south-Eastern Mediterranean, during the PreTECT campaign. Second, to demonstrate the feasibility of evaluation of desert dust transport model simulations using the detailed dust properties retrieved by the GRASP/GARRLiC. The NMME-DREAM dust model was analyzed in the current study.

Our study is organized as follows: Section 2 presents an overview of the PreTECT campaign and the Finokalia observatory. This section also presents the remote sensing instruments used, an overview of the retrieval algorithms applied herein and a brief description of the dust model NMME-DREAM. Section 3 presents the dust case analysis and the obtained results. Finally, Section 4 gives the main conclusions and perspectives.

## 2. Instrumentation and Methodology

### 2.1. The PreTECT Campaign and the Site of Finokalia

The PreTECT experimental campaign (<http://pre-TECT.space.noa.gr/>, accessed on 29 December 2020) was held at the northern coast of Crete, Greece, at the Finokalia research station (35°20' N, 25°40' E), during April 2017. A large consortium of European research institutes and universities participated in this combined effort, was organized by the National Observatory of Athens (NOA). The Finokalia station is located at the top of a hilly elevation (252m above sea level (a.s.l.)) facing the sea, far from human activities (more than 20 km distance). The site is representative of the regional conditions of the eastern Mediterranean [32] and is very often affected by long-range transported mineral dust from north Africa. Other aerosol types that are frequently observed are marine and smoke particles [33]. The PreTECT campaign is mainly focused on desert dust characterization, uses remote sensing measurements and applies advanced inversion techniques to derive the microphysical and optical properties of the particles.

### 2.2. Instruments and Tools

During the PreTECT campaign a large suite of remote sensing sensors was deployed at Finokalia, along with the in-situ instrumentation that regularly operates at the station. Unfortunately, for the case study presented here, no in-situ data were available. The instruments and tools used herein are described in detail below.

#### 2.2.1. PollyXT Lidar

The PollyXT lidar [34] of NOA is a multi-wavelength system that operated on an all day and night monitoring basis during the campaign, providing vertically resolved aerosol optical properties. PollyXT-NOA employs an Nd:YAG laser emitting linearly-polarized light at the primary wavelength of 1064 nm. The system is equipped with three elastic backscatter channels (at 355, 532 and 1064 nm), two rotational-vibrational Raman extinction channels (at 387 and 607 nm), two linear depolarization channels (at 355 and 532 nm), and one water vapor detection channel (at 407 nm). The receiver part of PollyXT-NOA is composed of a far-range and a near-range receiver with a full overlap height at ~200 m above ground, decreasing the minimal measurement height in the planetary boundary layer. The PollyXT-NOA lidar is part of the European Aerosol Research Lidar NETwork (EARLINET) [35], and the PollyNET network (portable Raman lidar systems) [36]. The derived products meet the EARLINET guidelines for data quality assurance [37].

#### 2.2.2. CIMEL Sun-Photometer

The CIMEL sun-photometer installed at the Finokalia station during the campaign, is part of the Aerosol Robotic Network (AERONET) [38] and was operated by NOA. The direct sun and sky measurements provide the aerosol optical depth (AOD) at eight wavelengths from 340 to 1640 nm, along with the products derived from the AERONET inversion algorithm [11,39]: the columnar volume size distribution, complex refractive index, single scattering albedo and the scattering phase function.

### 2.3. Retrieval Algorithms

#### 2.3.1. GRASP/GARRLiC Retrieval Algorithm

As briefly mentioned in the introduction, the main retrieval algorithm used in this study, the GRASP/GARRLiC inversion algorithm [18], combines lidar with sun-photometer measurements and provides the column-integrated and vertically resolved optical and microphysical properties of the aerosol particles in the atmosphere. GRASP/GARRLiC input consists of the sun-photometer sun and sky measurements and the elastic backscatter lidar signals, while different combinations of inputs/outputs are supported (e.g., [20,40]). As shown in Figure 1, in the current study we use as input the lidar measurements of elastic backscatter signals at 355, 532 and 1064 nm, and the sun-photometer measurements of AOD and of diffused light (up to 35 scattering angles) at 440, 670, 870 and 1020 nm. To

extend the lidar profiles as close to the ground as possible, we combined the information from lidar far-range and near-range receivers. Specifically, a gluing technique [41] on the lidar signal level was applied, extending the profiles at ~200 m above the ground.

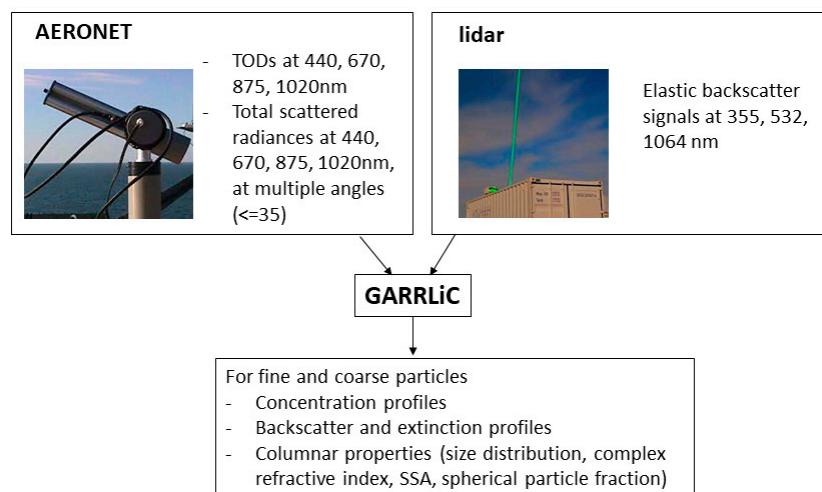


**Figure 1.** GRASP/GARRLiC algorithm input and output parameters.

The acquired optical and microphysical properties are derived for both fine and coarse mode particles. These are the aerosol volume concentration profiles and columnar microphysical and optical properties: the single scattering albedo (SSA), the particle size distribution, the real and imaginary part of refractive index (RRI and IRI, respectively) and the particle spherical fraction. GRASP/GARRLiC provides the possibility of a single-mode inversion as well for events dominated by a certain type of aerosol, as is the case in the present study.

Several conditions are required for the successful application of the GRASP/GARRLiC retrieval algorithm. The daytime sun-photometer data should be obtained in cloud-free atmospheric conditions. Moreover, it is preferable to use early-day measurements in order to avoid the sun background in lidar measurements. Moreover, high aerosol loading (AOD at 440 nm of 0.4 or greater) is desirable for reliable retrievals of aerosol absorption. Moreover, the retrieval uses the assumption of a plane-parallel atmosphere, and therefore only one averaged dataset of lidar profiles should be used. Furthermore, in the situations when one type of aerosol dominates the measurements, the default retrieval of two aerosol modes can be ambiguous and an assumption of a single aerosol mode is more appropriate [23].

### 2.3.2. POLIPHON Retrieval Algorithm

POLIPHON [42] uses single-wavelength lidar observations with one polarization-sensitive channel, and as such the method is simple and robust. POLIPHON performs the vertical separation of two to three particle components in different aerosol mixtures, deriving their optical properties and mass concentrations. The POLIPHON approach is designed explicitly to avoid the use of a particle shape model and a strong dependence on photometer observations, providing, however, a less complete suite of optical and microphysical products than GRASP/GARRLiC. The retrieval uses the particle linear depolarization ratio that separates the non-spherical particle contribution to the particle backscatter coefficient for a given wavelength. The AERONET observations are only used to provide with the aerosol-type-specific “mass-specific extinction coefficients” used in POLIPHON for the calculation of the mass concentration profiles.

For the dust case, the discrimination is performed for three components (POL-2 version) [14]: dust coarse, dust fine and non-dusty aerosols. For the case study herein, the latter component is expected to include marine and anthropogenic pollution.

## 2.4. NMME-DREAM Dust Model

NMME-DREAM is the dust model evaluated in this study. It consists of the meteorological core NCEP-NMME (Nonhydrostatic Mesoscale Model on E-grid) atmospheric model [43]. DREAM [44–46] is a numerical model developed to simulate and predict the atmospheric life cycle of mineral dust including dust emission, dust horizontal and vertical turbulent mixing, long-range transport and dust deposition, using an Euler-type nonlinear partial differential equation for dust mass continuity. The model is configured at  $0.2^\circ \times 0.2^\circ$  resolution and includes 8 dust size bins with effective radius of 0.15, 0.25, 0.45, 0.78, 1.3, 2.2, 3.8 and  $7.1 \mu\text{m}$  respectively. In the present study, 3 hourly instantaneous model outputs are used.

## 3. Results

### 3.1. Characterization of the Dust Event of 14 May 2017

The dust event that took place at Finokalia on 14 May 2017 is shown in Figure 2a presents the total attenuated backscatter coefficient from the lidar measurements at 1064 nm, depicting the vertical extend of the plume that reaches up to  $\sim 5$  km, while there is also a thin layer at  $\sim 6$ – $7$  km. The volume linear depolarization ratio (VLDR) values at 532 nm exceed 15%, which indicates the presence of non-spherical particles from  $\sim 0.5$  up to 5 km. Lower VLDR values below 500 m can be attributed to a possible mixture of dust with marine particles. The AERONET product also indicates the presence of dust particles, with a high aerosol load ( $\text{AOD} \approx 0.7$  at 440 nm) and an Angstrom exponent at 440/870 nm of  $\sim 0.14$ , with the latter within the range of the climatological values for desert dust [47].

Total Attenuated Backscatter coefficient at 1064 nm, PollyXT NOAA, Finokalia, 14/5/2017

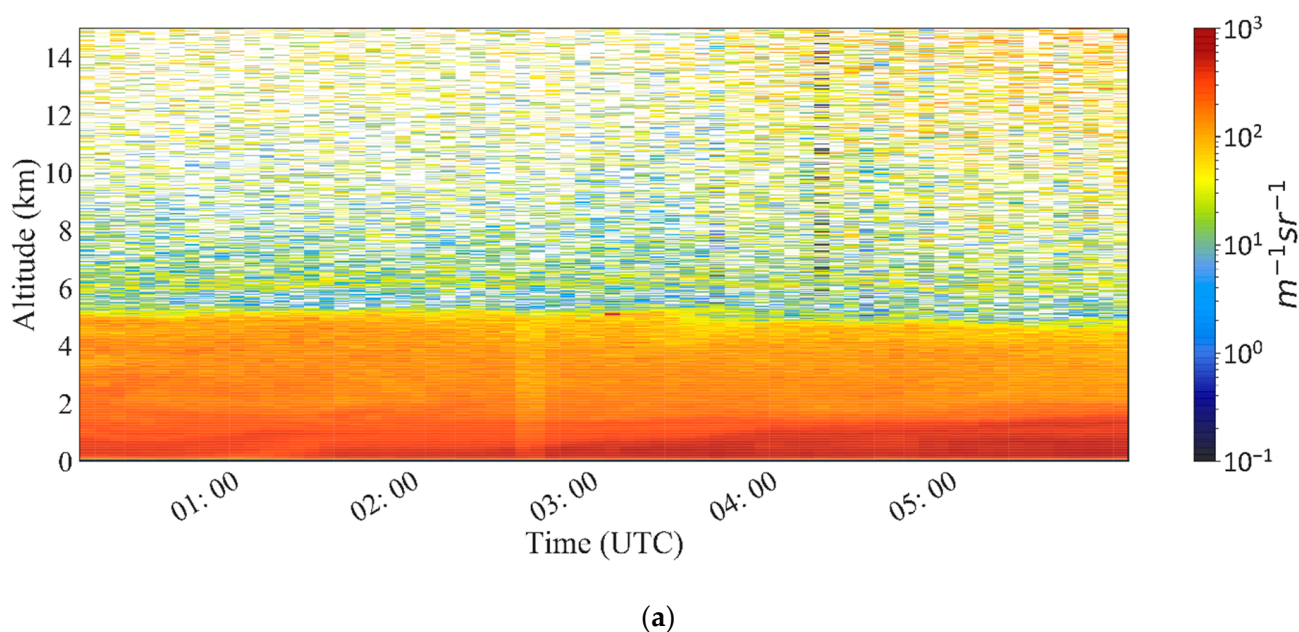
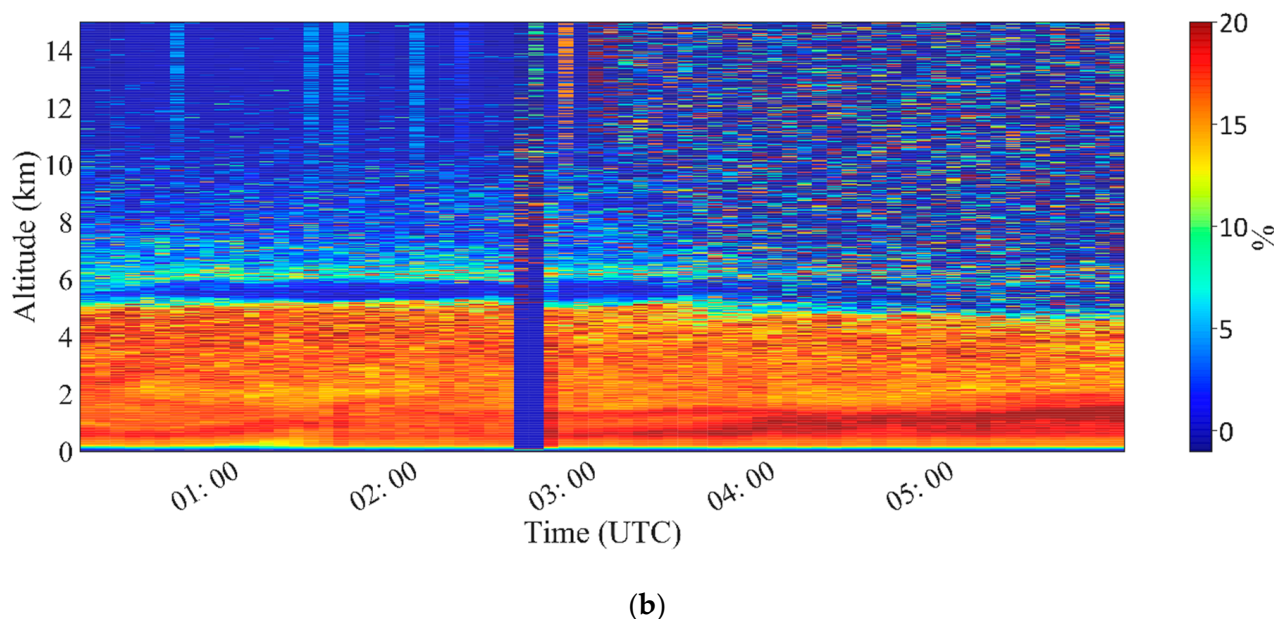


Figure 2. Cont.



## Volume Linear Depolarization Ratio at 532 nm, PollyXT NOA, Finokalia, 14/5/2017



**Figure 2.** Time-height cross section of the (a) range-corrected backscattered signal at 1064 nm in arbitrary units and (b) volume depolarization ratio (%) measured from PollyXT NOA lidar on 14 May 2017, over Finokalia, Greece.

To determine the origin of the particles, we perform back-trajectory analysis using the atmospheric dispersion model FLEXPART-WRF [48]. The 24-h backtrajectories (Figure 3a) show that the air masses arriving at 3 to 10 km above Finokalia, have followed a westerly flow originating from the Sahara region (Tunisia and Algeria), while in the origins for the air-masses arriving below 2 km, sources include the Ionian Sea and the northern part of Greece, suggesting possible contributions from marine and anthropogenic aerosols. The forecast of the NMME-DREAM dust model on 12 May 2017 (Figure 3b) confirms the origin of mineral dust from Algeria and Tunisia and the transport path through the Mediterranean.

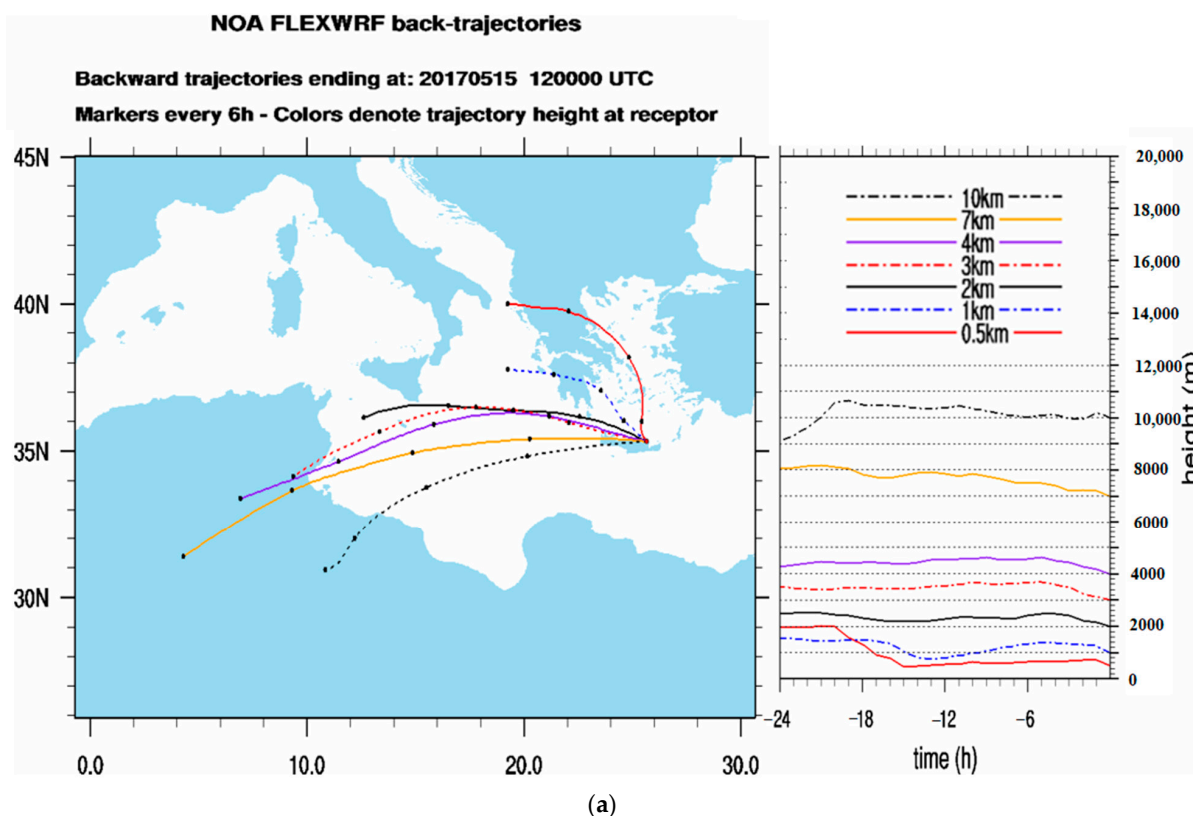


**Figure 3.** Cont.

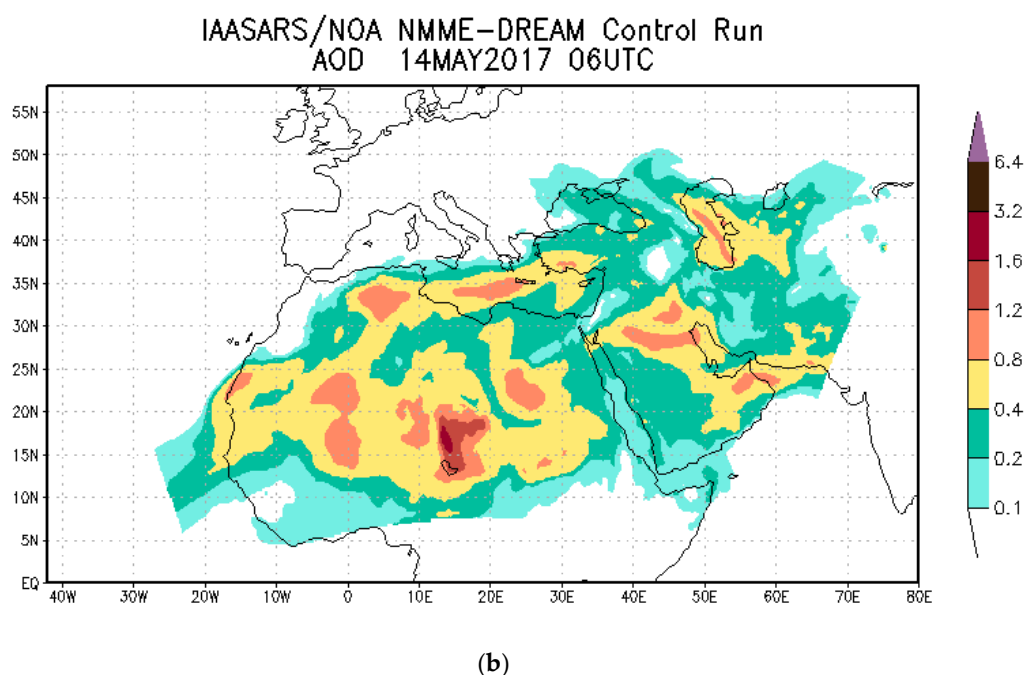


**Figure 3.** (a) 24 h backward-trajectories from FLEXPART-WRF over different heights at Finokalia station at 12:00 UTC and (b) dust optical depth (DOD) values forecasted by NMME-DREAM dust model over Africa and Europe at 06:00 UTC on 14 May 2017.

### 3.2. Retrieval of Dust Properties

We characterized the dust plume on 14 May 2017 with the GRASP/GARRLiC retrieval, using the lidar measurements at 05:00–06:00 UTC (red box in Figure 2), and the sun-photometer measurements at 05:52 UTC. The AERONET volume size distribution (black line in Figure 4) exhibits a predominant coarse mode, and thus the single-mode inversion (i.e., without retrieving separated values for fine and coarse modes) is performed.

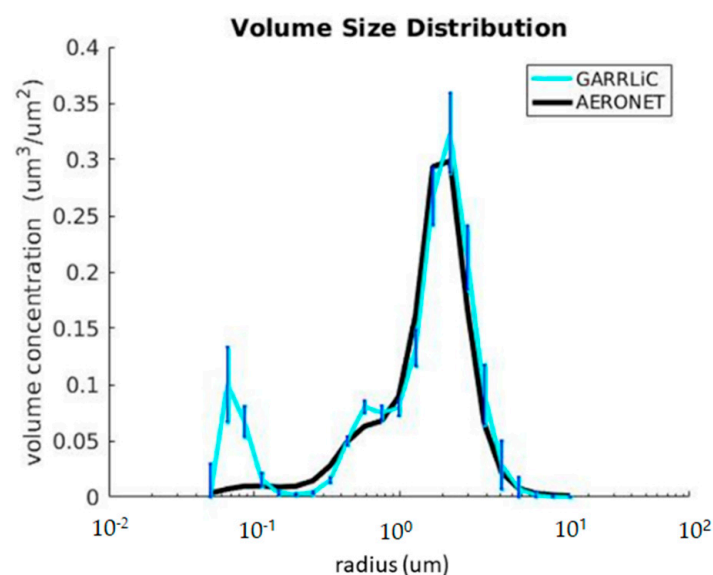


**Figure 4.** The volume size distribution retrieved from GRASP/GARRLiC (blue line) and from AERONET (black line), on 14 May 2017, over Finokalia, Greece.

Blue lines in Figures 4–6 present the retrieved aerosol columnar microphysical properties from GRASP/GARRLiC (i.e., volume size distribution, refractive index and SSA), all in comparison with the AERONET retrievals (black lines) for this case study. The error bars

in the plots denote the variability of the GRASP/GARRLiC retrieval for different input settings, and not the retrieval errors. The GRASP/GARRLiC and AERONET retrievals show good agreement for the size distribution of large dust particles (Figure 4), but not for the smaller ones, which are almost absent in the AERONET retrieval.

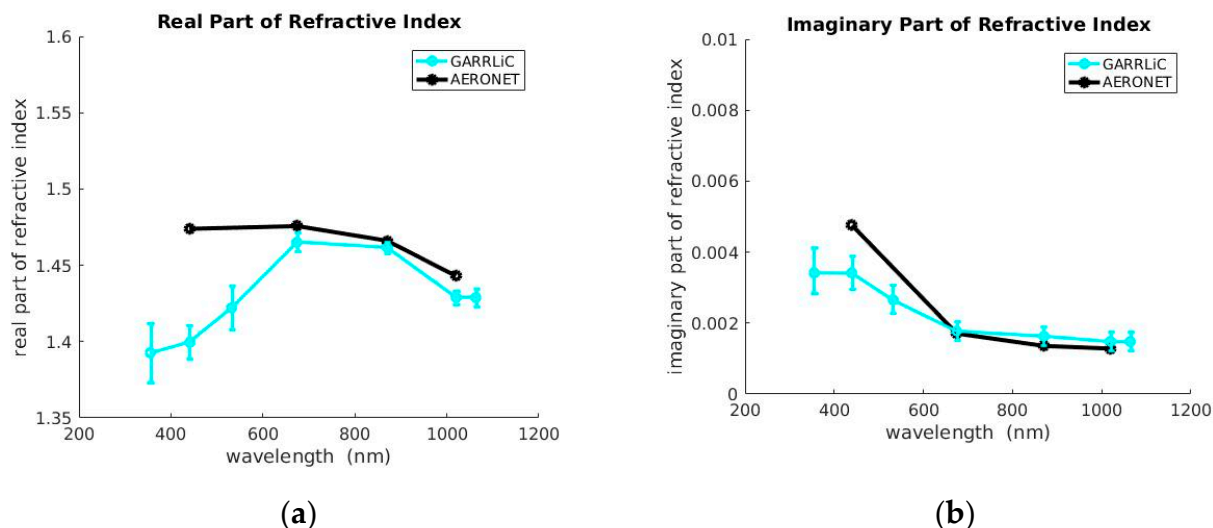


**Figure 5.** (a) Real and (b) imaginary part of refractive index retrieved from GRASP/GARRLiC (blue line) and from AERONET (black line), on 14 May 2017, over Finokalia, Greece.

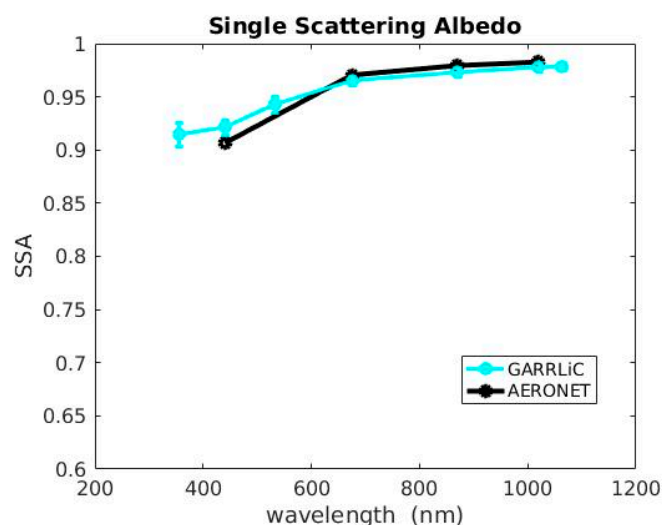


**Figure 6.** Single scattering albedo retrieved from GRASP/GARRLiC (blue line) and from AERONET (black line), on 14 May 2017, over Finokalia, Greece.

The real part of the refractive index (RRI, Figure 5a) provided by GRASP/GARRLiC agrees well with the AERONET values for wavelengths  $>670$  nm, while for smaller wavelengths the first is much lower than the latter. The range of the RRI is  $\sim 1.4$ – $1.45$ , which is at the low end of the climatological values for dust [47]. These values indicate that dust is probably mixed with marine particles, with a typical value for RRI of  $\sim 1.36$ , as discussed also in [23]. The same holds true for the values of the imaginary part of refractive index (CRI, Figure 5b), which ranges from 0.003 to 0.002 from the UV to the Near-IR.

The SSA increases with increasing wavelength, from 0.92 at 440 nm to 0.98 at 1020 nm, and is in good agreement with the AERONET retrieval (Figure 6). These values are also indicative of the presence of dust particles [47,49].



Figure 7 shows the vertical profiles of the particle backscatter and extinction coefficients at 355 and 532 nm retrieved from lidar measurements with the Klett method [50] (blue and green dashed lines for 355 and 532 nm, respectively), and with the GRASP/GARRLiC algorithm (blue and green solid lines for 355 and 532 nm, respectively). For the Klett retrievals, we used a lidar ratio of 67.5 sr and 56 sr at 355 and 532 nm, respectively, so that the integral of the retrieved extinction coefficient profiles closely reproduce the AOD measured by the sun-photometer at 340 and 500 nm. Moreover, we used the glued signals from lidar far-range and near-range receivers. The resulting particle extinction and backscatter coefficient profiles retrieved with the Klett method and GRASP/GARRLiC are found to be in reasonable agreement, with the GRASP/GARRLiC values being slightly smaller, in the order of  $\sim 3\%$  compared to the values retrieved with the Klett method. These differences may arise from the different assumptions of the profile behavior near the ground for the two methods: GRASP/GARRLiC assumes it to be constant at the lowest 200 m, which is not the case for the Klett method. The GRASP/GARRLiC particle extinction and backscatter coefficient profiles are much smoother due to the reduced resolution of the lidar signals, which is suggested for reducing lidar signal noise levels and the complexity of the retrieval [18].

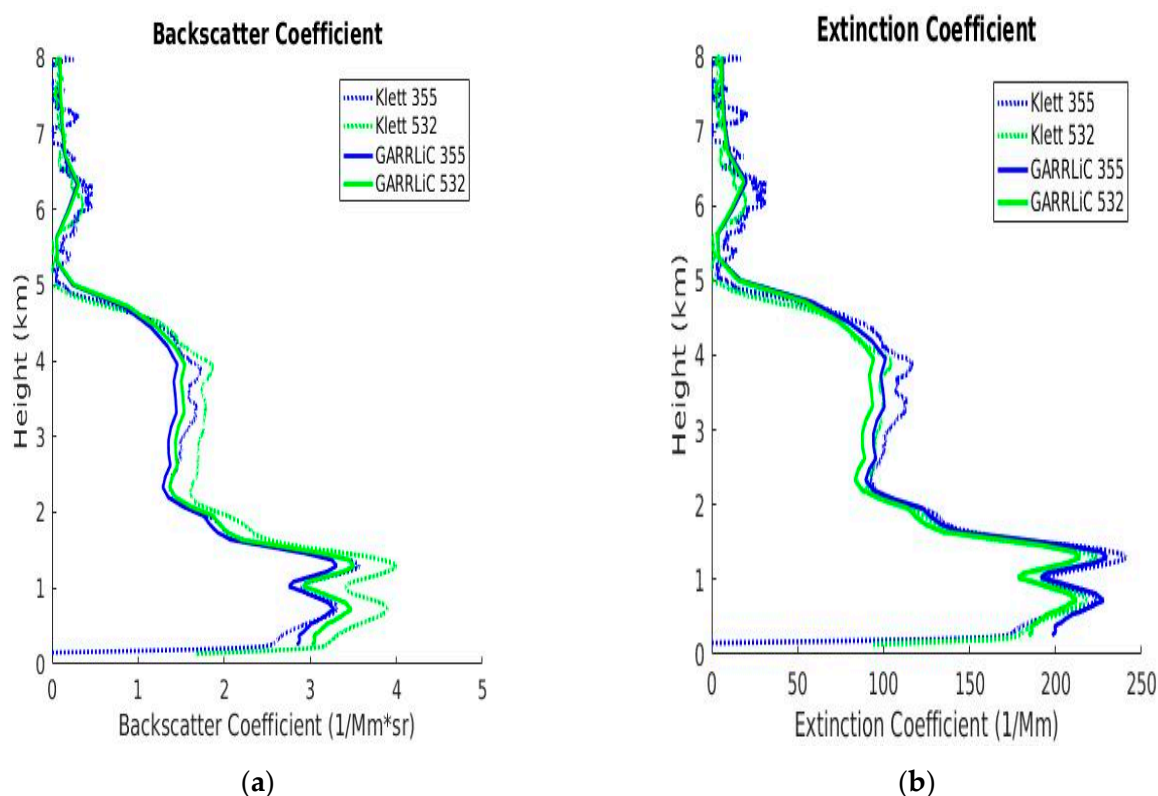


**Figure 7.** The (a) backscatter and (b) extinction coefficients at 355 and 532 nm, retrieved with the Klett method (dash lines), and the corresponding retrieved profiles from GRASP/GARRLiC (solid lines), for the dust event of 14 May 2017, over Finokalia.

### 3.3. Comparison between Retrieved and Simulated Dust Concentration Profiles

In Figure 8 the aerosol mass concentration profile retrieved with GRASP/GARRLiC (blue line) is compared with the corresponding profile simulated with the NMME-DREAM model (black line). For the conversion of the volume concentration profile provided by GRASP/GARRLiC, to the corresponding mass concentration profile, we consider that all particles have a density of  $2.35 \text{ g/cm}^3$ , which is the mean of the  $2.1\text{--}2.6 \text{ g/cm}^3$  density range provided in the literature for dust [51]. The error bars in the GRASP/GARRLiC mass concentration profile in Figure 8 denote this density range.

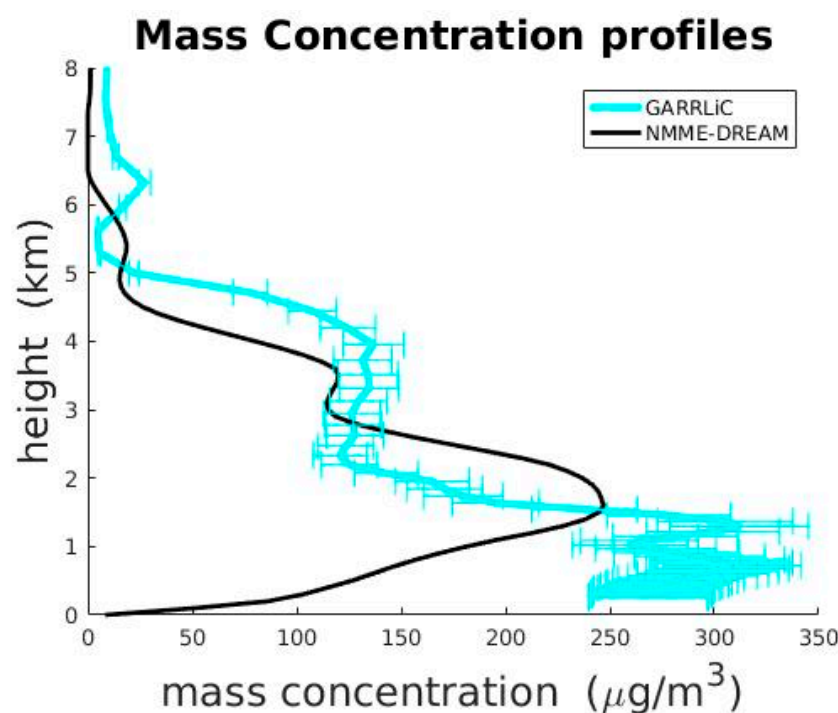


**Figure 8.** The mass concentration profiles retrieved with GRASP/GARRLiC algorithm (blue line) and the dust mass concentration profile simulated by NMME-DREAM (black line) for the dust event of 14 May 2017, over Finokalia, Greece. The error bars for the GRASP/GARRLiC retrieval denote the density range of 2.1–2.6 g/cm<sup>3</sup> used for the conversion of the volume to mass concentrations.

The NMME-DREAM model predicts two concentration peaks in the dust plume: one at 3.5 km with a concentration of  $\sim 130 \mu\text{g}/\text{m}^3$  and one at 2 km with a concentration of  $\sim 250 \mu\text{g}/\text{m}^3$ , revealing the models' biases when compared with the GRASP/GARRLiC retrievals for this specific episode. The mass concentration values retrieved by GRASP/GARRLiC from the surface up to 2 km are strongly underestimated by the model; GRASP/GARRLiC retrieval presents a maximum concentration of  $300 \mu\text{g}/\text{m}^3$  at  $\sim 1.5$  km, while the NMME-DREAM model profile quickly declines from the max concentration of  $\sim 250 \mu\text{g}/\text{m}^3$  at 2 km to low concentration values of  $50 \mu\text{g}/\text{m}^3$  closer to the surface. The model's behavior of underestimating dust concentrations at low altitudes is consistent with the findings of previous studies [10,23,30]. At higher layers (above 2 km) dust concentration decreases with height up to 5 km, while an optically thin layer located between 5.5 and 7 km is also depicted by GRASP/GARRLiC retrieval. The model overestimates concentrations between 1.5 to 3 km and underestimates them between  $\sim 3$  to 5 km height.

#### 4. Discussion

The comparison between GRASP/GARRLiC retrievals and the NMME-DREAM model dust concentration profiles suggests an under-prediction of the actual dust concentrations in the model for the dust episode under study. The poor representation of the boundary layer of the dust event is probably due to the low resolution of the model that makes it difficult to capture the topography in detail with the continental mountainous ranges. These features may play an important role in the model's dynamics and the downward winds that have a very local nature and can cause mixing of dust concentrations induced by the complex topography [10].

To strengthen the above results, the mass concentration profiles simulated with a NMME-DREAM model and retrieved with GRASP/GARRLiC are compared with the mass concentration profiles retrieved with POLIPHON (Figure 9) for continental (green dashed line), dust (magenta dashed line) and marine particles (blue dashed line). For the POLIPHON retrieval we used only the far range signals, since there is no near-range cross-

polarized measurements. Figure 9 shows that the POLIPHON algorithm also indicates the limited presence of other aerosols types compared to dust, at heights above  $\sim 1$  km and finds the maximum peak for dust particles at 2 km at high concentration values of  $350 \mu\text{g}/\text{m}^3$ , thus enhancing GRASP/GARRLiC retrievals.

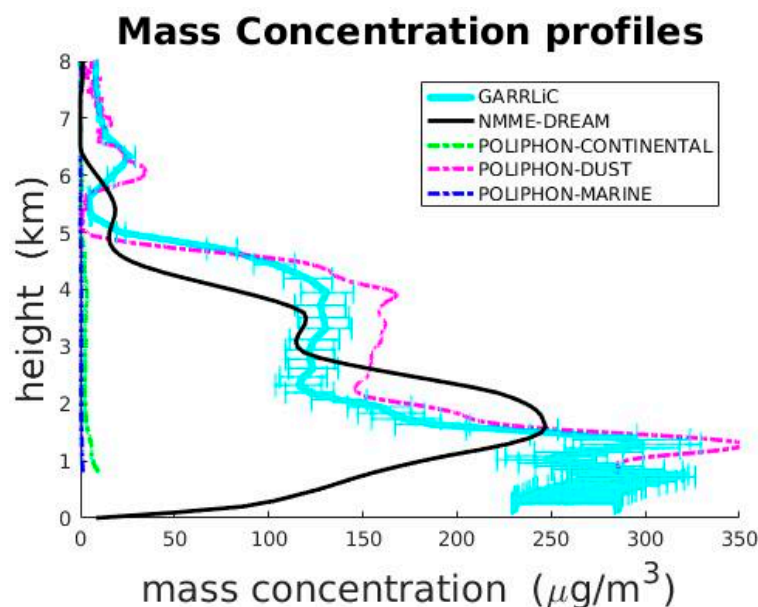


**Figure 9.** Comparison of particle concentration profiles retrieved with GRASP/GARRLiC algorithm (blue line) and simulated by NMME-DREAM (black line), as in Figure 8, compared with POLIPHON retrievals for continental (green dashed line), dust (magenta dashed line) and marine particles (blue dashed line), for the dust event of 14 May 2017, over Finokalia, Greece.

## 5. Conclusions

This study applies the GRASP/GARRLiC inversion algorithm to coincident EARLINET lidar and AERONET sun-photometer observations performed at the Finokalia station in Crete during the PreTECT campaign. The algorithm was applied during an intense Saharan dust episode on 14 May 2017 reaching  $256 \mu\text{g}/\text{m}^3$  at 250 m and derived columnar dust properties, in terms of the particle size distribution, spectral complex refractive index and SSA, as well as the concentration profiles. The GRASP/GARRLiC retrieval agrees well with the AERONET product for the larger particles, and with climatological values of dust.

A second objective of this study was to demonstrate a high potential value of dust concentration profiles retrieved by GRASP/GARRLiC for evaluation of the dust model simulations (NMME-DREAM is used for this case study). Additionally, the retrievals from the POLIPHON technique were used to estimate the mass concentration profile and enhance the driven conclusions. The GRASP/GARRLiC retrievals agree reasonably well with the model simulations at high altitudes for this dust episode, with both capturing the maximum dust concentrations at 2 km ( $250 \mu\text{g}/\text{m}^3$  for GRASP/GARRLiC and  $300 \mu\text{g}/\text{m}^3$  for the model) but at the lower layers ( $\sim 1$ – $2$  km) the model strongly underestimates dust concentrations. This underestimation at low levels is in accordance with POLIPHON retrieved mass concentrations that further confirm that there is no other dominant type of aerosols but dust at these heights. Below 1 km, we expect the contribution of the marine particles, but the lack of near-range cross-polarized measurements does not facilitate their retrieval with POLIPHON.

The selected event of 14 May 2017 is characterized by a two-peak vertical structure that is adequately reproduced by the model, but also by concentrations up to  $300 \mu\text{g}/\text{m}^3$  inside the PBL that are not reproduced. Similar limitations have been previously reported for mesoscale simulations at the station of Finokalia in Crete, due to the inaccurate repre-

sentation of local dynamics that are induced by the sharp topography of the island [10]. Nevertheless, the comparison contributes to the systematic use of the sun-photometer/lidar synergy in GRASP/GARRLiC to model-evaluation studies.

Overall, the present study showed that GRASP/GARRLiC is an innovative proposition for remote sensing microphysical retrievals based on synergies of sophisticated ground-based sensors applied within the frame of the ACTRIS Research Infrastructure. Within this framework, real time ACTRIS GRASP/GARRLiC data that will be automatically retrieved from raw lidar data from the EARLINET, combined with coincident AERONET data are under development. Moreover, the algorithm is continuously tested and improved to reach an automation mature state for future application in satellite platforms.

**Author Contributions:** Conceptualization, D.K., V.A., A.T. and P.N.; methodology, D.K., A.T., and S.S.; software, D.K., S.S., N.S., A.G. and E.T.; validation, A.T., S.S., A.L., P.G. and O.D.; formal analysis, D.K., N.S., A.G. and E.T.; investigation, D.K., A.T. and S.S.; resources, V.A. and P.N.; data curation, D.K.; writing—original draft preparation, D.K.; writing—review and editing, A.T., S.S., A.L., P.G., O.D., V.A. and P.N.; visualization, D.K.; supervision, A.T., V.A. and P.N.; project administration, V.A.; funding acquisition, P.N. and V.A. All authors have read and agreed to the published version of the manuscript.

**Funding:** This research was funded by 1. the project “PANhellenic infrastructure for Atmospheric Composition and climatE change” (MIS 5021516) which is implemented under the Action “Reinforcement of the Research and Innovation Infrastructure”, funded by the Operational Programme “Competitiveness, Entrepreneurship and Innovation” (NSRF 2014-2020) and co-financed by Greece and the European Union (European Regional Development Fund). 2. the ERC Consolidator Grant 2016 D-TECT: “Does dust TriboElectrification affect our ClimaTe?” (grant no. 725698). 3. the Stavros Niarchos Foundation (SNF). 4. O. Dubovik and P. Goloub appreciate support from the Chemical and Physical Properties of the Atmosphere Project funded by the French National Research Agency through the Programme d’Investissement d’Avenir under contract ANR-11-LABX-0 0 05-01, the Regional Council “Hauts-de-France”, and the “European Funds for Regional Economic Development”.

**Institutional Review Board Statement:** Not applicable.

**Informed Consent Statement:** Not applicable.

**Data Availability Statement:** Publicly available datasets were analyzed in this study. This data can be found here: <http://pre-TECT.space.noa.gr/> (accessed on 29 December 2020).

**Conflicts of Interest:** The authors declare no conflict of interest. The funders had no role in the design of the study; in the collection, analyses, or interpretation of data; in the writing of the manuscript, or in the decision to publish the results.

## References

1. Balkanski, Y.; Schulz, M.; Claquin, T.; Guibert, S. Reevaluation of Mineral aerosol radiative forcings suggests a better agreement with satellite and AERONET data. *Atmos. Chem. Phys.* **2007**, *7*, 81–95. [\[CrossRef\]](#)
2. DeMott, P.J.; Sassen, K.; Poellot, M.R.; Baumgardner, D.; Rogers, D.C.; Brooks, S.D.; Prenni, A.J.; Kreidenweis, S.M. African dust aerosols as atmospheric ice nuclei, *Geophys. Res. Lett.* **2003**, *30*, 1732. [\[CrossRef\]](#)
3. Morman, S.A.; Plumlee, G.S. Dust and human health. In *Mineral Dust*; Knippertz, P., Stuut, J.-B.W., Eds.; Springer: Dordrecht, The Netherlands, 2014; pp. 385–409.
4. Nastos, P.T.; Paliatatos, A.G.; Anthracopoulos, M.B.; Roma, E.S.; Priftis, K.N. Outdoor particulate matter and childhood asthma admissions in Athens, Greece: A time-series study. *Environ. Health* **2010**, *9*, 45. [\[CrossRef\]](#) [\[PubMed\]](#)
5. Nastos, P.T.; Kampanis, N.A.; Giaouzaki, K.N.; Matzarakis, A. Environmental impacts on human health during a Saharan dust episode at Crete Island, Greece. *Meteorol. Z.* **2011**, *20*, 517–529. [\[CrossRef\]](#)
6. Nastos, P.T.; Bleta, A.G.; Matsangouras, I.T. Human thermal perception related to Föhn winds due to Saharan dust outbreaks in Crete Island, Greece. *Theor. Appl. Climatol.* **2017**, *128*, 635–647. [\[CrossRef\]](#)
7. Kaskaoutis, D.G.; Kosmopoulos, P.G.; Nastos, P.T.; Kambezidis, H.D. Manish Sharma and Waseem Mehdi: Transport pathways of Sahara dust over Athens, Greece as detected by MODIS and TOMS, *Geomatics. Nat. Haz. Risk* **2012**, *3*, 35–54. [\[CrossRef\]](#)
8. Moulin, C.; Lambert, C.E.; Dayan, U.; Masson, V.; Ramonet, M.; Bousquet, P.; Legrand, M.; Balkanski, Y.J.; Guelle, W.; Marticorena, B.; et al. Satellite climatology of African dust transport in the Mediterranean atmosphere. *J. Geophys. Res.* **1998**, *103*, 13137–13144. [\[CrossRef\]](#)



9. Kallos, G.; Astitha, M.; Katsafados, P.; Spyrou, C. Long-range transport of anthropogenically and naturally produced particulate matter in the Mediterranean and North Atlantic: Current state of knowledge. *J. Appl. Meteorol. Climatol.* **2007**, *46*, 1230–1251. [\[CrossRef\]](#)
10. Solomos, S.; Kalivitis, N.; Mihalopoulos, N.; Amiridis, V.; Kouvarakis, G.; Gkikas, A.; Biniotoglou, I.; Tsekeri, A.; Kazadzis, S.; Kottas, M.; et al. From Tropospheric Folding to Khamsin and Foehn Winds: How Atmospheric Dynamics Advanced a Record-Breaking Dust Episode in Crete. *Atmosphere* **2018**, *9*, 240. [\[CrossRef\]](#)
11. Dubovik, O.; King, M.D. A flexible inversion algorithm for retrieval of aerosol optical properties from sun and sky radiance measurements. *J. Geophys. Res.* **2000**, *105*, 20673–20696. [\[CrossRef\]](#)
12. Dubovik, O.; Herman, M.; Holdak, A.; Lapyonok, T.; Tanre, D.; Deuze, J.L.; Ducos, F.; Sinyuk, A.; Lopatin, A. Statistically optimized inversion algorithm for enhanced retrieval of aerosol properties from spectral multi-angle polarimetric satellite observations. *Atmos. Meas. Tech.* **2011**, *4*, 975–1018. [\[CrossRef\]](#)
13. Nisantzi, A.; Mamouri, R.E.; Ansmann, A.; Schuster, G.; Hadjimitsis, D. Middle East versus Saharan dust extinction-to-backscatter ratios. *Atmos. Chem. Phys.* **2015**, *15*. [\[CrossRef\]](#)
14. Mamouri, R.-E.; Ansmann, A. Potential of polarization/Raman lidar to separate fine dust, coarse dust, maritime, and anthropogenic aerosol profiles. *Atmos. Meas. Tech.* **2017**, *10*, 3403–3427. [\[CrossRef\]](#)
15. Marinou, E.; Amiridis, V.; Biniotoglou, I.; Tsikerdekis, A.; Solomos, S.; Proestakis, E.; Konsta, D.; Papagiannopoulos, N.; Tsekeri, A.; Vlastou, G.; et al. Three-dimensional evolution of Saharan dust transport towards Europe based on a 9-year EARLINET-optimized CALIPSO dataset. *Atmos. Chem. Phys.* **2017**, *17*, 5893–5919. [\[CrossRef\]](#)
16. Chaikovsky, A.; Dubovik, O.; Goloub, P.; Tanré, D.; Pappalardo, G.; Wandinger, U.; Chaikovskaja, L.; Denisov, S.; Grudo, Y.; Lopatsin, A.; et al. Algorithm and software for the retrieval of vertical aerosol properties using combined lidar/radiometer data: Dissemination in EARLINET. In Proceedings of the 26th International Laser Radar Conference, Porto Heli, Greece, 25–29 June 2015.
17. Chaikovsky, A.; Dubovik, O.; Holben, B.; Bril, A.; Goloub, P.; Tanre, D.; Pappalardo, G.; Wandinger, U.; Chaikovskaya, L.; Denisov, S.; et al. Lidar-Radiometer Inversion Code (LIRIC) for the retrieval of vertical aerosol properties from combined lidar/radiometer data: Development and distribution in EARLINET. *Atmos. Meas. Tech.* **2016**, *9*, 1181–1205. [\[CrossRef\]](#)
18. Lopatin, A.; Dubovik, O.; Chaikovsky, A.; Goloub, P.; Lapyonok, T.; Tanre, D.; Litvinov, P. Enhancement of aerosol characterization using synergy of lidar and sun-photometer coincident observations: The GARRLiC algorithm. *Atmos. Meas. Tech.* **2013**, *6*, 2065–2088. [\[CrossRef\]](#)
19. Dubovik, O.; Lapyonok, T.; Litvinov, P.; Herman, M.; Fuertes, D.; Ducos, F.; Lopatin, A.; Chaikovsky, A.; Torres, B.; Derimian, Y.; et al. *GRASP: A Versatile Algorithm for Characterizing the Atmosphere*; SPIE: Bellingham, DC, USA, 2014.
20. Bovchaliuk, V.; Goloub, P.; Podvin, T.; Veselovskii, I.; Tanre, D.; Chaikovsky, A.; Dubovik, O.; Mortier, A.; Lopatin, A.; Korenskiy, M.; et al. Comparison of aerosol properties retrieved using GARRLiC, LIRIC, and Raman algorithms applied to multi-wavelength lidar and sun/sky-photometer data. *Atmos. Meas. Tech.* **2016**, *9*, 3391–3405. [\[CrossRef\]](#)
21. Parajuli, S.P.; Stenchikov, G.L.; Ukhov, A.; Shevchenko, I.; Dubovik, O.; Lopatin, A. Interaction of Dust Aerosols with Land/Sea Breezes over the Eastern Coast of the Red Sea from LIDAR Data and High-resolution WRF-Chem Simulations. *Atmos. Chem. Phys. Discuss.* **2020**. [\[CrossRef\]](#)
22. Lopatin, A.; Dubovik, O.; Fuertes, D.; Stenchikov, G.; Lapyonok, T.; Veselovskii, I.; Wienhold, F.G.; Shevchenko, I.; Hu, Q.; Parajuli, S. Synergy processing of diverse ground-based remote sensing and in situ data using GRASP algorithm: Applications to radiometer, lidar and radiosonde observations. *Atmos. Meas. Tech. Discuss.* **2020**. [\[CrossRef\]](#)
23. Tsekeri, A.; Lopatin, A.; Amiridis, V.; Marinou, E.; Igloffstein, J.; Siomos, N.; Solomos, S.; Kokkalis, P.; Engelmann, R.; Baars, H.; et al. GARRLiC and LIRIC: Strengths and limitations for the characterization of dust and marine particles along with their mixtures. *Atmos. Meas. Tech.* **2017**, *10*, 4995–5016. [\[CrossRef\]](#)
24. Benavent-Oltra, J.A.; Román, R.; Granados-Muñoz, M.J.; Pérez-Ramírez, D.; Ortiz-Amezcuca, P.; Denjean, C.; Lopatin, A.; Lyamani, H.; Torres, B.; Guerrero-Rascado, J.L.; et al. Comparative assessment of GRASP algorithm for a dust event over Granada (Spain) during ChArMEx-ADRIMED 2013 campaign. *Atmos. Meas. Tech.* **2017**, *10*, 4439–4457. [\[CrossRef\]](#)
25. Román, R.; Benavent-Oltra, J.A.; Casquero-Vera, J.A.; Lopatin, A.; Cazorla, A.; Lyamani, H.; Denjean, S.; Fuertes, D.; Pérez-Ramírez, D.; Torres, B.; et al. Retrieval of aerosol profiles combining sunphotometer and ceilometer measurements in GRASP code. *Atmos. Res.* **2018**, *204*, 161–177. [\[CrossRef\]](#)
26. Kezoudi, M.; Tesche, M.; Smith, H.; Tsekeri, A.; Baars, H.; Dollner, M.; Estellés, V.; Weinzierl, B.; Ulanowski, Z.; Müller, D.; et al. Measurement report: Balloon-borne in-situ profiling of Saharan dust over Cyprus with the UCASS optical particle counter. *Atmos. Chem. Phys. Discuss.* **2020**. [\[CrossRef\]](#)
27. Heinold, B.; Helmert, J.; Hellmuth, O.; Wolke, R.; Ansmann, A.; Marticorena, B.; Laurent, B.; Tegen, I. Regional modeling of Saharan dust events using LM-MUSCAT: Model description and case studies. *J. Geophys. Res.* **2007**, *112*, D11204. [\[CrossRef\]](#)
28. Amiridis, V.; Wandinger, U.; Marinou, E.; Giannakaki, E.; Tsekeri, A.; Basart, S.; Kazadzis, S.; Gkikas, A.; Taylor, M.; Baldasano, J.; et al. Optimizing CALIPSO Saharan dust retrievals. *Atmos. Chem. Phys.* **2013**, *13*, 12089–12106. [\[CrossRef\]](#)
29. Tsekeri, A.; Amiridis, V.; Kokkalis, P.; Basart, S.; Chaikovsky, A.; Dubovik, O.; Mamouri, R.E.; Papayannis, A.; Baldasano, J.M. Application of a Synergetic Lidar and Sunphotometer Algorithm for the Characterization of a Dust Event Over Athens, Greece. *Br. J. Environ. Clim. Chang.* **2013**, *3*, 531–546. [\[CrossRef\]](#)



30. Biniotoglou, I.; Basart, S.; Alados-Arboledas, L.; Amiridis, V.; Argyrouli, A.; Baars, H.; Baldasano, J.M.; Balis, D.; Belegante, L.; Bravo-Aranda, J.A.; et al. A methodology for investigating dust model performance using synergistic EARLINET/AERONET dust concentration retrievals. *Atmos. Meas. Tech.* **2015**, *8*, 3577–3600. [\[CrossRef\]](#)
31. Konsta, D.; Biniotoglou, I.; Gkikas, A.; Solomos, S.; Marinou, E.; Proestakis, E.; Basart, S.; Perez Garcia-Pando, C.; Amiridis, V.; El-Askary, H. Evaluation of the BSC-DREAM8b regional dust model using the 3D LIVAS-CALIPSO product. *Atmos. Environ.* **2018**, *195*, 46–62. [\[CrossRef\]](#)
32. Lelieveld, J.; Berresheim, H.; Borrmann, S.; Crutzen, P.J.; Dentener, F.J.; Fischer, H.; Feichter, J.; Flatau, P.J.; Heland, J.; Holzinger, R.; et al. Global air pollution crossroads over the Mediterranean. *Science* **2002**, *298*, 794–799. [\[CrossRef\]](#) [\[PubMed\]](#)
33. Pikridas, M.; Bougiatioti, A.; Hildebrandt, L.; Engelhart, G.J.; Kostenidou, E.; Mohr, C.; Prevot, A.S.H.; Kouvarakis, G.; Zampas, P.; Burkhardt, J.F.; et al. The Finokalia Aerosol Measurement Experiment—2008 (FAME-08): An overview. *Atmos. Chem. Phys. Discuss.* **2010**, *10*, 1–39.
34. Engelmann, R.; Kanitz, T.; Baars, H.; Heese, B.; Althausen, D.; Skupin, A.; Wandinger, U.; Komppula, M.; Stachlewska, I.S.; Amiridis, V.; et al. The automated multiwavelength Raman polarization and water-vapor lidar Polly XT: The neXT generation. *Atmos. Meas. Tech.* **2016**, *9*, 1767–1784. [\[CrossRef\]](#)
35. Bosenberg, J.; Ansmann, A.; Baldasano, J.; Balis, D.; Böckmann, C.; Calpini, B. EARLINET: A European Aerosol Research Lidar Network. In Proceedings of the 20th international Laser Radar Conference (ILRC), Vichi, France, 8–13 November 2000.
36. Baars, H.; Kanitz, T.; Engelmann, R.; Althausen, D.; Heese, B.; Komppula, M.; Preißler, J.; Tesche, M.; Ansmann, A.; Wandinger, U.; et al. An overview of the first decade of PollyNET: An emerging network of automated Raman-polarization lidars for continuous aerosol profiling. *Atmos. Chem. Phys.* **2016**, *16*, 5111–5137. [\[CrossRef\]](#)
37. Freudenthaler, V.; Linné, H.; Chaikovski, A.; Rabus, D.; Groß, S. EARLINET lidar quality assurance tools. *Atmos. Meas. Tech. Discuss.* **2018**. [\[CrossRef\]](#)
38. Holben, B.N.; Eck, T.F.; Slutsker, I.; Tanre, D.; Buis, J.P.; Setzer, A.; Vermote, E.; Reagan, J.A.; Kaufman, Y.J.; Nakajima, T.; et al. AERONET-A federated instrument network and data archive for aerosol characterization. *Remote Sens. Environ.* **1998**, *66*, 1–16. [\[CrossRef\]](#)
39. Dubovik, O.; Sinyuk, A.; Lapyonok, T.; Holben, B.N.; Mishchenko, M.; Yang, P.; Eck, T.F.; Volten, H.; Muñoz, O.; Veihelmann, B.; et al. Application of spheroid models to account for aerosol particle nonsphericity in remote sensing of desert dust. *J. Geophys. Res.* **2006**, *111*, D11208. [\[CrossRef\]](#)
40. Hu, Q.; Goloub, P.; Veselovskii, I.; Bravo-Aranda, J.-A.; Popovici, I.E.; Podvin, T.; Haefelin, M.; Lopatin, A.; Dubovik, O.; Pietras, C.; et al. Long-range-transported Canadian smoke plumes in the lower stratosphere over northern France. *Atmos. Chem. Phys.* **2019**, *19*, 1173–1193. [\[CrossRef\]](#)
41. D’Amico, G.; Amodeo, A.; Mattis, I.; Freudenthaler, V.; Pappalardo, G. EARLINET Single Calculus Chain—technical—Part 1: Pre-processing of raw lidar data. *Atmos. Meas. Tech.* **2016**, *9*, 491–507. [\[CrossRef\]](#)
42. Mamouri, R.E.; Ansmann, A. Fine and coarse dust separation with polarization lidar. *Atmos. Meas. Tech.* **2014**, *7*, 3717–3735. [\[CrossRef\]](#)
43. Janjic, Z.I.; Gerrity, J.P., Jr.; Nickovic, S. An Alternative Approach to Nonhydrostatic Modeling. *Mon. Weather Rev.* **2001**, *129*, 1164–1178. [\[CrossRef\]](#)
44. Nickovic, S.; Kallos, G.; Papadopoulos, A.; Kakaliagou, O. A model for prediction of desert dust cycle in the atmosphere. *J. Geophys. Res.* **2001**, *106*, 18113–18129. [\[CrossRef\]](#)
45. Nickovic, S.; Cvetkovic, B.; Madonna, F.; Rosoldi, M.; Pejanovic, G.; Petkovic, S.; Nikolic, J. Cloud ice caused by atmospheric mineral dust—Part 1: Parameterization of ice nuclei concentration in the NMME-DREAM model. *Atmos. Chem. Phys.* **2016**, *16*, 11367–11378. [\[CrossRef\]](#)
46. Solomos, S.; Abuelgasim, A.; Spyrou, C.; Biniotoglou, I.; Nickovic, S. Development of a dynamic dust source map for NMME-DREAM v1.0 model based on MODIS Normalized Difference Vegetation Index (NDVI) over the Arabian Peninsula. *Geosci. Model Dev.* **2019**, *12*, 979–988. [\[CrossRef\]](#)
47. Dubovik, O.; Holben, B.; Eck, T.; Smirnov, A.; Kaufman, Y.; King, M.; Tanre, D.; Slutsker, I. Variability of absorption and optical properties of key aerosol types observed in worldwide locations. *J. Atmos. Sci.* **2002**, *59*, 590–608. [\[CrossRef\]](#)
48. Brioude, J.; Arnold, D.; Stohl, A.; Cassiani, M.; Morton, D.; Seibert, P.; Angevine, W.; Evan, S.; Dingwell, A.; Fast, J.D.; et al. The Lagrangian particle dispersion model FLEXPARTWRF version 3.1. *Geosci. Model Dev.* **2013**, *6*, 1889–1904. [\[CrossRef\]](#)
49. Otto, S.; De Reus, M.; Trautmann, T.; Thomas, A.; Wendisch, M.; Borrmann, S. Atmospheric radiative effects of an in situ measured Saharan dust plume and the role of large particles. *Atmos. Chem. Phys.* **2007**, *7*, 4887–4903. [\[CrossRef\]](#)
50. Klett, D. Lidar inversion with variable backscatter/extinction ratios. *Appl. Optics* **1985**, *31*, 1638–1643. [\[CrossRef\]](#) [\[PubMed\]](#)
51. Reid, J.S.; Jonsson, H.H.; Maring, H.B.; Smirnov, A.; Savoie, D.L.; Cliff, S.S.; Reid, E.A.; Livingston, J.M.; Meier, M.M.; Dubovik, O.; et al. Comparison of size and morphological measurements of coarse mode dust particles from Africa. *J. Geophys. Res. Atmos.* **2003**, *108*, 8593. [\[CrossRef\]](#)